

© 2022 This manuscript version is made available under the CC-BY-NC-ND 4.0 license
<https://creativecommons.org/licenses/by-nc-nd/4.0/>

The definitive publisher version is available online at
<https://doi.org/10.1016/j.jenvman.2022.114463>

1 **Water treatment sludge conversion to biochar as**
2 **cementitious material in cement composite**

3
4 Samuel De Carvalho Gomes^a, John L. Zhou^{a,b}, Xiaohui Zeng^b, Guangcheng Long^b

5
6 ^aCenter for Green Technology, School of Civil and Environmental Engineering, University
7 of Technology Sydney, NSW 2007, Australia

8 ^bSchool of Civil Engineering, Central South University, Changsha, Hunan Province,
9 410075, China

10
11
12
13 Corresponding author:

14 Prof. John. Zhou, Email: junliang.zhou@uts.edu.au

15 **Abstract**

16 Water treatment sludge was successfully thermally converted to obtain biochar as a stable
17 material with resource potential. This research explored the application of sludge biochar as a
18 supplementary cementitious material. The cement paste samples incorporating different
19 amounts of sludge biochar were prepared, hardened, and analyzed for performance. The results
20 show an improvement in hydration kinetics and mechanical properties of cement paste
21 incorporating biochar, compared to raw sewage sludge. The mineralogical, thermal and
22 microscopic analyses show evidence of pozzolanic activity of the biochar. The samples with
23 2% and 5% biochar showed higher heat release than the reference material. Specimens with
24 1%, 2% and 5% biochar showed a slightly higher compressive strength at 28 days compared to
25 the reference material. Sludge conversion to biochar will incur an estimated cost of
26 US\$398.23/ton, which is likely to be offset by the substantial benefits from avoiding landfill
27 and saving valuable cementitious materials. Therefore, this research has demonstrated that
28 through conversion to biochar, water treatment sludge can be promoted as a sustainable and
29 alternative cementitious material for cement with minimum environmental impacts, hence
30 contributing to circular economy.

31

32 *Keywords:* Water treatment sludge; Biochar; Cement composites; Hydration kinetics;
33 Structural performance

34 **1. Introduction**

35 Water treatment plants are playing a critically important role worldwide to purify raw water for
36 human consumption (Chang et al., 2020). During the water treatment processes, chemical
37 reagents such as coagulants and flocculants are added for the removal of fine particles and
38 dissolved organic matter such as humic substances (Ahmed et al., 2018; Huang et al., 2020;
39 Van Truong et al., 2021), leading to the formation of particle residues that will be removed in
40 later stages by screening, sedimentation and filtration (Manda et al., 2016; Shamaki et al.,
41 2021). These solid residues are commonly known as water treatment sludge, which is produced
42 in enormous quantity e.g. 43500 ton/y in Australia (Gomes et al., 2020) and causes major
43 environmental pollution if discharged directly to rivers (Hussein et al., 2021). Therefore, water
44 treatment sludge is usually dewatered and sent to landfill sites (Gomes et al., 2019). However,
45 with increasingly stringent legislation and high disposal costs, as well as the potential
46 environmental impacts associated with improper disposal and landfill leachate (Yadav et al.,
47 2020), both water treatment companies and local governments are seeking more economic and
48 sustainable solutions for the long-term management of water treatment sludge (Teodosiu et al.,
49 2018).

50 Currently, the search for solutions to minimize the adverse environmental impacts of solid
51 waste and landfill practices has led to the development of research into the use of water
52 treatment sludge as a potential resource. Many studies have been carried out to recover the
53 chemical coagulants used during the water purification process and to directly use such sludge
54 as coagulants in parts of the wastewater treatment process (Taheriyoun et al., 2020; Letshwenyo
55 and Mokgosi, 2021). More recently, another area that has been extensively explored is the
56 incorporation of such sludge in different construction materials such as bricks (Erdogmus et al.,
57 2021), concrete paving blocks (Liu et al., 2020), lightweight aggregates (Lee et al., 2021;
58 Mañosa et al., 2021b), mortar (Li et al., 2021), alkali-activated cements (Mañosa et al., 2021a),
59 and geopolymers (Gomes et al., 2019; Santos et al., 2019), as clay and sludge have a similar

60 mineralogical composition. As construction materials are in high demand globally, the potential
61 use of water treatment sludge in construction industry will greatly reduce material cost, improve
62 their environmental credentials, and make their contributions towards circular economy
63 (Shamaki et al., 2021).

64 Up to now, most research has used raw sludge which is mixed with other materials (Gomes
65 et al., 2020), or in some cases the sludge has been calcined before its incorporation (Benlalla et
66 al., 2015; de Godoy et al., 2019). More recently, there has been research work investigating the
67 possibility of recycling and valorizing water treatment sludge into a rich-carbon based material
68 called biochar through pyrolysis (Lee et al., 2020; Hung et al., 2020). Biochar is a carbon-rich
69 material obtained from carbonized biomass under a low oxygen atmosphere, with half of the
70 carbon content from the original organic compounds (Ahmed et al., 2016; Mulabagal et al.
71 2017). Biochar commonly presents more stabilized carbon concentration than the original raw
72 material; hence, the carbon contained in biochar is less likely to be released back into the
73 atmosphere as carbon dioxide. Therefore, the motivation for biochar use stems from its unique
74 properties (e.g. porosity, surface area, surface charge) and diverse applications in fields such as
75 waste management, energy production, climate change mitigation and soil improvement, which
76 individually or in combination can have very positive environmental and socio-economic
77 effects (Lehmann, 2007; Steiner et al., 2008; Beesley et al., 2010). Recent research shows that
78 the incorporation of only 1% biochar substitution could sequester approximately 0.5 Gt of CO₂
79 annually by the concrete industry, approximately 20% of the entire annual CO₂ released by
80 cement industry (Di Tommaso and Bordonzotti, 2016). Similarly, Gupta and Kua (2017)
81 suggested that by using biochar in construction materials to capture and then lock atmospheric
82 carbon dioxide in buildings and structures can potentially reduce 25% of greenhouse gas
83 emissions from the construction industry.

84 There has been a growing interest in the use of biochar as cementitious materials to improve
85 its mechanical performance. Akhtar and Sarmah (2018) investigated the substitution of cement

86 by 1% biochar produced from different raw materials (poultry waste, rice hulls and sludge from
87 pulp and paper mills). Their results revealed that the biochar of pulp-paper sludge obtained
88 compressive strength similar to the control sample. Interestingly, the replacement of only 0.1%
89 of rice husk biochar increased the tensile and flexural strengths of concrete by 20% comparing
90 with the control samples. Using biochar made from wood and sawdust at 300 °C and 500 °C,
91 Gupta et al. (2018) showed that the addition of 2% biochar in the mortar mixture offered a
92 significant improvement in the compressive and flexural strength of the composite. In addition,
93 the permeability of the composite was significantly reduced due to the addition of biochar, due
94 to the effect of biochar as a micro-filler in the mortar.

95 There is some recent research on the application of biochar from different sources in
96 Portland cement, however so far, there is still no published study, to our knowledge, on the
97 application of biochar prepared from water treatment sludge as an ingredient of cement
98 composites. Therefore, the application of water treatment sludge biochar in cement paste is the
99 novelty of this study. The comparison of raw sludge and sludge biochar in their structural
100 performance as a cement paste is a further novelty. In order to improve the valorization of water
101 treatment sludge as an ingredient to the construction industry, this research aimed to prepare
102 sludge biochar, characterize biochar for key physicochemical properties, determine the
103 mechanical strengths of fresh and hardened cement paste incorporating different contents of
104 sludge biochar, and analyze the impacts and interaction of sludge biochar on the hydration
105 kinetics of cement products.

106

107 **2. Materials and methods**

108 *2.1. Raw materials*

109 The water treatment sludge was collected from the Cascade Water Filtration Plant at Katoomba,
110 NSW, Australia, where ferric chloride (FeCl_3) was used as the coagulant in its conventional
111 water treatment process. The dewatered sludge was collected from the drying bed at four

112 different points. The sludge was dried in an oven at 105 °C for 24 h to remove the moisture,
113 following procedures recommended by the American Society for Testing and Materials
114 (ASTM, 2020). The dried sludge was then crushed, sieved (300 µm) and stored in an airtight
115 plastic bag before further characterization (**Fig. A1a, Supplementary Information**).

116 The cement used in the study was a general purpose (GP) cement from Cement Australia,
117 which fully complies with the Australian Standard AS 3972 (2010). The cement has a density
118 of 3.0-3.2 g/cm³, with a median particle size of 9.4 mm.

119

120 *2.2. Biochar preparation from water treatment sludge*

121 The naturally dried and sieved sludge was used to prepare biochar. In brief, the sludge was
122 placed inside a fixed bed reactor (**Fig. A1b, Supplementary Information**) which was then
123 inserted into a furnace (Labec). Pyrolysis was operated in a furnace at 700 °C for 2 h, with the
124 temperature increase rate of 17 °C/min. To maintain a low oxygen atmosphere and prevent
125 oxidation during the process, the nitrogen gas was injected to the reactor at a flow rate of 220
126 mL/min. The biochar samples were then cooled at room temperature until reaching a constant
127 weight (**Fig. A1c, Supplementary Information**).

128

129 *2.3. Cement composite testing*

130 To examine the feasibility of sludge and sludge biochar application as supplementary
131 cementitious material, sludge or sludge biochar was mixed with cement to prepare cement
132 composites. Briefly, GP cement was mixed with different amount of sludge or sludge biochar
133 (1%, 2%, 5%, 10%) based on the weight of the cement (**Table 1**). In addition, reference cement
134 paste was prepared with no biochar addition. In order to ensure full hydration, cement paste
135 was cast with water to cement ratio of 0.4, according to the Standard C305-14 (ASTM, 2014).

136 For the compressive strength test, twelve specimens of cubic moulds (50 mm × 50 mm ×
137 50 mm) were cast for each mixture design. After demolding, the blended pastes were cured at

138 20 °C under 95% relative humidity and tested at 7, 14, and 28 days respectively. Compressive
 139 strength testing was conducted in accordance with the Standard C109-16 (ASTM, 2016), which
 140 provides a means of determining the compressive strength of hydraulic cement and other
 141 mortars. The compression testing was conducted on a Universal Hydraulic Test Frame (UH-
 142 500kN XR) with a REH50 load frame (Shimadzu).

143 The heat of hydration of the composite pastes was determined using an I-Cal 4000
 144 isothermal calorimeter (Calmetrix), in accordance with the Standard C1679 (ASTM, 2009). All
 145 the mixtures were prepared by hand for 30 s, from which 25 g of the paste was used for each
 146 cup mixture test. All measurements were performed during the first 48 h of hydration at a
 147 controlled temperature of 20 °C.

148

149 **Table 1.** The experimental design of different cement paste mixtures.

Mixture	Cement (g)	Sludge or biochar (g)	Water (g)	Water/binder ratio
Reference	2800	0	1120	0.4
Sludge (1%)	2800	28	1120	0.4
Sludge (2%)	2800	56	1120	0.4
Sludge (5%)	2800	140	1120	0.4
Sludge (10%)	2800	280	1120	0.4
Biochar (1%)	2800	28	1120	0.4
Biochar (2%)	2800	56	1120	0.4
Biochar (5%)	2800	140	1120	0.4
Biochar (10%)	2800	280	1120	0.4

150

151 *2.4. Characterization of materials and cement paste*

152 The composite samples containing different amounts of sludge or the sludge-derived biochar
 153 were subjected to extensive characterization. The thermal gravimetric-differential scanning
 154 calorimetry (TG-DSC) analysis was performed using a Simultaneous Thermal Analyzer (model

155 STA 449 F5 Jupiter). The powder from the composite pastes of 28 days curing were collected
156 by cracking blended pastes and immediately immersed into ethyl alcohol for 24 h and dried at
157 40 °C overnight. The simultaneous thermogravimetry used the nitrogen gas at a gas velocity of
158 20 mL/min. The 28-day powder samples were heated from 30 °C to 900 °C at a rate of 20
159 °C/min.

160 X-ray diffraction (XRD) analysis was used to identify the mineralogical characterization of
161 sludge biochar and the hydration evolution of the composite at early-age hydration, the XRD
162 analyses were performed by using a Bruker D8 Discover diffractometer. The fine powder from
163 28 days curing was subjected to the XRD apparatus at 20 mA and 40 kV, scanned within a 2θ
164 range of 5° to 55°.

165 The morphology of the sludge biochar and hydration products of composite was observed
166 by scanning electron microscope (SEM-EDS and Mapping) to examine the surface structure of
167 composite past samples. The fractured cement paste cubes (28 days) from the compressive
168 strength test were used. Prior to the analyses, the samples were dried at 40 °C for 24 h, then
169 coated with gold before examination in a Zeiss Supra 55VP SEM operated at 20 kV.

170

171 *2.5. Biochar cost analysis*

172 The full cost-benefit analysis of biochar production is highly important to support business
173 strategy and exploitation of biochar as a valuable product, which is not the focus of this study.
174 To prove the concept, the biochar production cost from sewage sludge is estimated, by
175 considering both capital investment cost and operating cost, following approaches reported by
176 Ahmed et al. (2016) and Nematian et al. (2021). The following cost analysis is based on a pilot
177 plant of biochar, with one ton per day of biochar production.

$$178 \quad C_P = C_{CI} + C_{OC} \quad (1)$$

179 where C_P is the overall production cost, C_{CI} is the total capital investment, C_{OC} is the total
180 operating cost, all in US\$/ton. The detailed breakdown of each cost has been described by

181 Ahmed et al. (2016). In addition, the calculation of total biochar production was estimated using
182 a biochar budget tool proposed by Nematian et al. (2021).

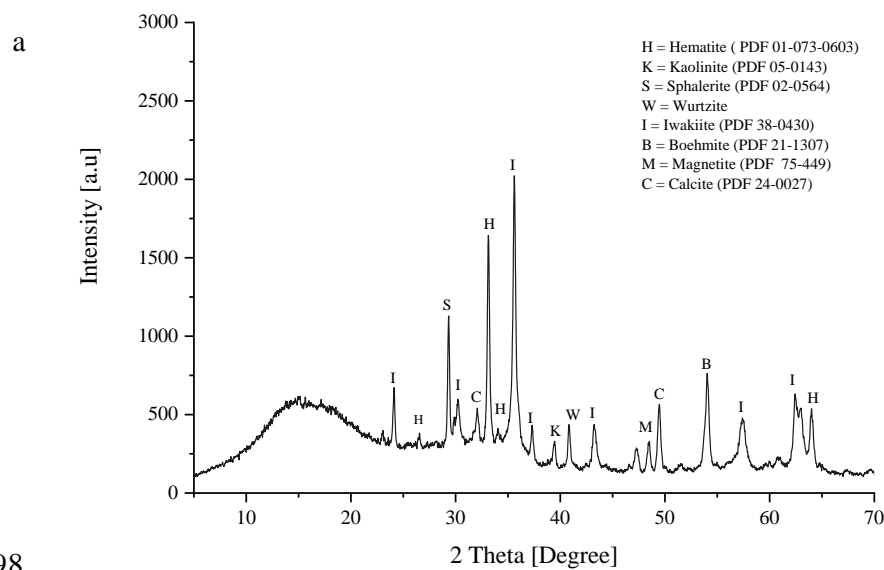
183

184 3. Results and discussion

185 3.1. Characterization of sludge biochar

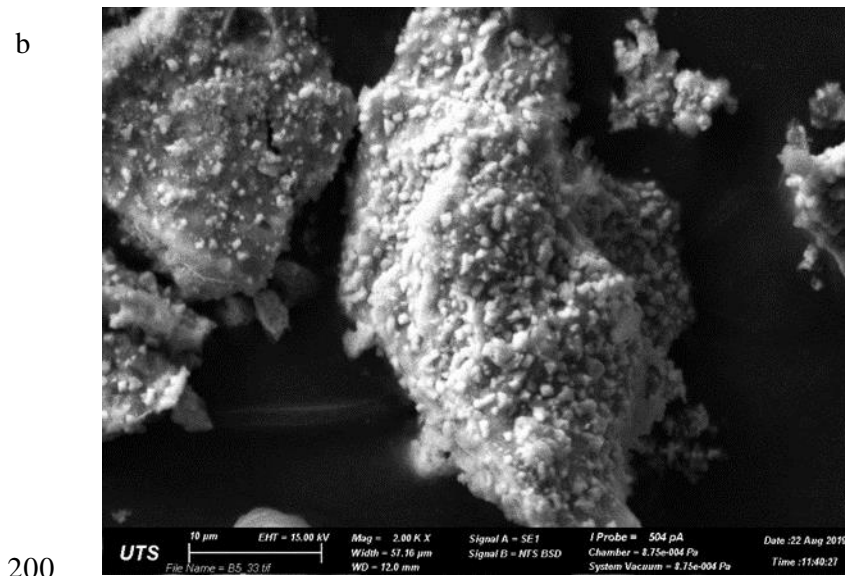
186 The XRD analysis of sludge biochar (**Fig. 1a**) shows a material with more crystalline peaks
187 than the raw sludge (Gomes et al., 2020). Most of the peaks detected were formed by the
188 dehydroxylation and conversion of iron oxides (goethite, ferrihydrite) in hematite and
189 magnetite (Teixeira et al., 2011; Kizinievič et al., 2013; Özdemir and Dunlop, 2000). The XRD
190 pattern shows the presence of wurtzite (ZnO), which was the convention of natural sphalerite
191 presented on the raw water treatment sludge (Hamza et al., 2017). Furthermore, the presence of
192 iwakiite (MnFe₂O₄) type is evident in the XRD profile, which is probably due to transformation
193 reaction between manganese and iron oxides, as described by Rzepa et al. (2016). Boehmite
194 has been detected due to partial dehydration of amorphous aluminum oxides (Tantawy et al.,
195 2015). The single peak of kaolinite is indicative of the dehydroxylation transformation of the
196 crystalline phase into amorphous metakaolin (Kakali et al., 2001; de Godoy et al., 2019).

197



198

199



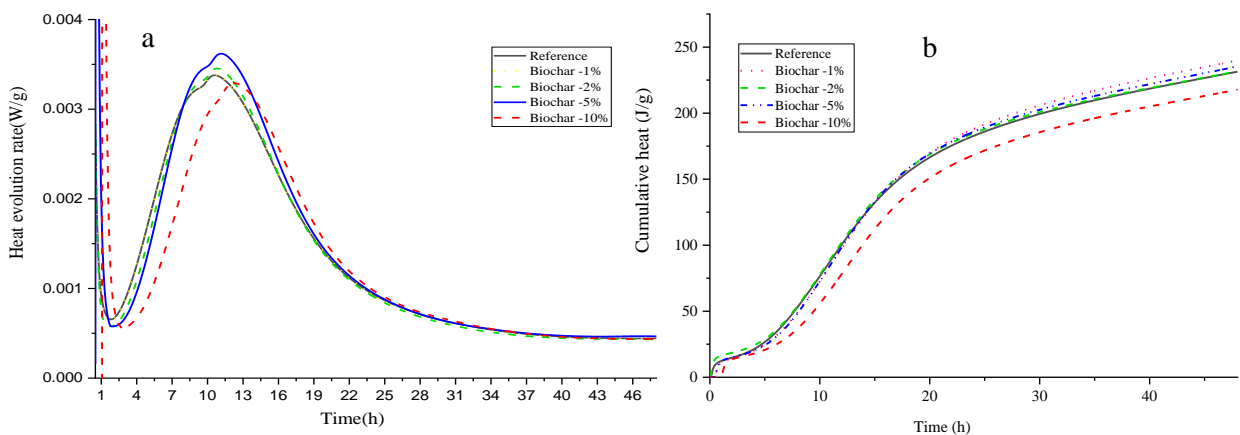
201 **Figure 1.** (a) The mineralogical composition of biochar from XRD analysis, and (b) SEM of
 202 biochar (2000 ×).
 203

204 The morphology of biochar from sludge preparation was examined by SEM (**Fig. 1b**). As
 205 can be shown, after the thermal pyrolysis process, the sludge grains underwent a significant
 206 transformation in their structure. In general, non-homogeneous particles with development
 207 rough texture and small clusters on the surface can be observed (San Nicolas et al., 2013; de
 208 Godoy et al., 2019).
 209

210 3.2. Heat evolution of cement paste

211 During the mixing of cement, aggregate and water, significant amounts of heat are released due
 212 to the exothermic nature of chemical reactions (i.e. hydration), which increase the temperature
 213 and maturing of concrete. **Figure 2** shows the heat evolution pattern by cement paste samples
 214 with different substitution of sludge biochar. The samples with 2% and 5% of sludge biochar
 215 released more heat than both the reference sample and 10% of sludge biochar addition. The
 216 initial peak (first h) is associated with the hydration of C_3A , the dissolution of free lime and the
 217 wetting of Portland cement, and all mixtures had similar results. However, the mixture with
 218 10% sludge biochar showed slightly more heat than the reference. The dormant stage (phase 2)

219 occurred during the first 2-3 hours of reaction for the reference samples (cement only). As the
 220 sludge biochar was added to the cement paste, this dormant period increased, reaching 5 hours
 221 concerning the samples with 10% sludge biochar. Similar to the reference sample, the curve
 222 with 1% sludge biochar showed two peaks, with the same intensity. These two peaks correspond
 223 to the rapid hydration of C_3S and C_3A respectively, followed by a deceleration period of heating.
 224 The mixtures with 2% and 5% of sludge biochar also showed two peaks but both with higher
 225 intensity compared to the reference and 1% biochar batches. This phenomenon is possibly
 226 associated with the filler surface effect, providing additional nucleation sites for calcium silicate
 227 hydrate (C-S-H) (Scrivener et al., 2015). The addition of 10% sludge biochar shows almost the
 228 same hydration heat compared to the reference, but with around 2 hours of delay in the reaction.
 229 It is important to note that the sludge biochar has shown improved hydration heat properties of
 230 the cement composites compared to the water treatment sludge itself (Gomes et al., 2020). For
 231 example, even the sample with the addition of 10% biochar had a similar heat peak compared
 232 to the reference sample, which did not happen with samples with the same proportion of raw
 233 sludge even at 48 h. In addition, another substantial improvement is the time delay in the
 234 maximum peak (formation of inner C-S-H) which has been reduced to 12.5 h with 10% biochar
 235 addition, compared to 38 h for 10% raw sludge addition. In other words, the addition of 10%
 236 sludge biochar caused only 2 h of delay for the maximum peak compared to the reference
 237 sample.



238 **Figure 2.** (a) Hydration heat evolution flow, and (b) cumulative heat evolution with the
 239 additions of different amounts of sludge biochar.

240

241 *3.3. Compressive strength of sludge biochar composite*

242 Concrete is used as a structure material; thus, its mechanical strengths should be fully tested.

243 The changes in comprehensive strength of cement paste samples over different curing time are

244 examined (**Fig. 3a**). At seven days of curing, mixtures with biochar showed slightly lower

245 compressive strength than the reference material, with 18.3% less compressive strengths when

246 10% biochar was added. However, there was a significant increase in the compressive strength

247 of the biochar composite over 28 days of curing. The mixtures with 1%, 2% and 5% sludge

248 biochar showed a slightly higher compressive strength at 28 days compared to the reference

249 material. Even with the addition of 10% sludge biochar, the cement paste presented a

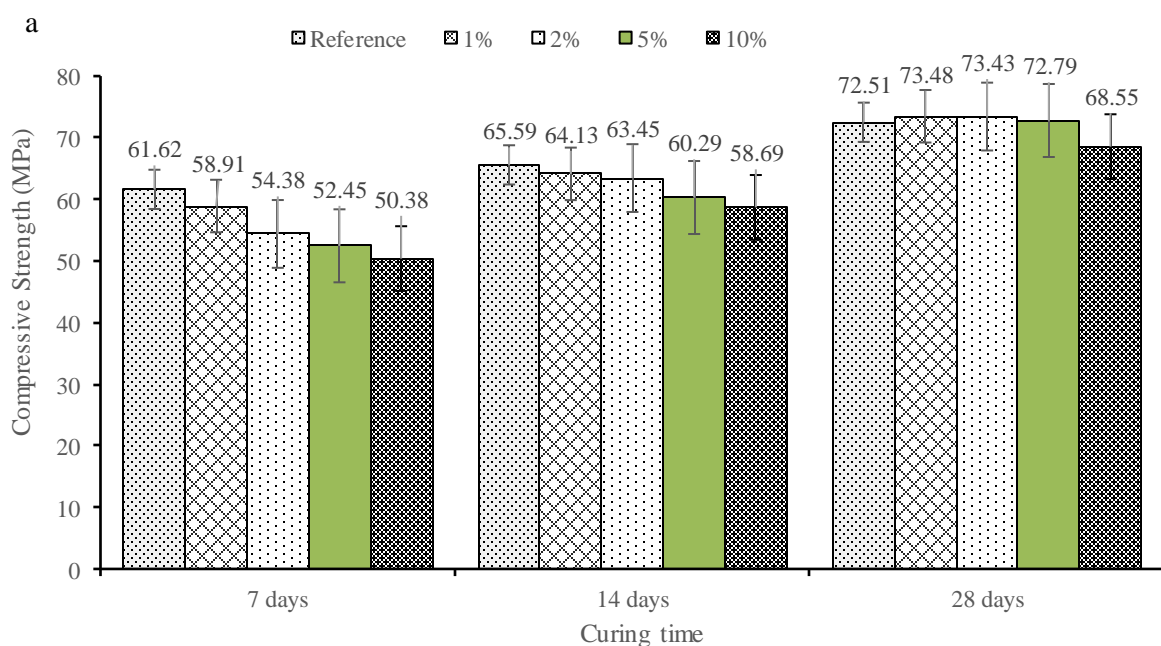
250 comprehensive strength value close to that of the reference material, with only 5.5% less

251 strength than the reference material with 100% cement. The analysis of variances (ANOVA)

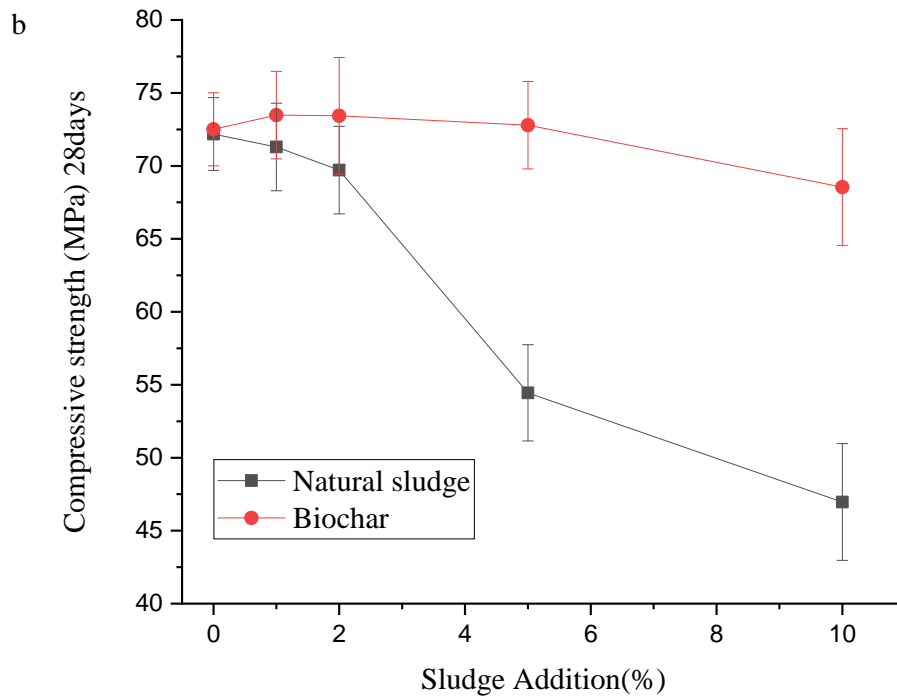
252 indicates that there is no statistical difference between the reference sample and any biochar composite

253 samples, at the end of 28 days of curing. The findings therefore confirm that up to 10% biochar can be

254 safely used to maintain the structural performance of cement paste.



255



256

257 **Figure 3.** (a) Compressive strength of cement paste with different amounts of sludge biochar.

258 (b) Comparison of compressive strength of cement paste at 28 days between water treatment
 259 sludge and sludge biochar.

260

261 Regarding the results at 28 days of curing, **Fig. 3b** compares the compressive strength
 262 between the composites of natural sludge and sludge biochar. For the additions of 5% and 10%
 263 sludge biochar, there was a significant increase in the compressive strength of 37% and 46%
 264 respectively, compared to the composite with natural sludge. This improvement in the
 265 behaviour of the biochar material was mainly due to the removal of organic matter in raw sludge
 266 through the thermal treatment, and also possibly the pozzolanic activity of biochar, even in
 267 small proportion at 28 days (Kaish et al., 2018; de Godoy et al., 2019).

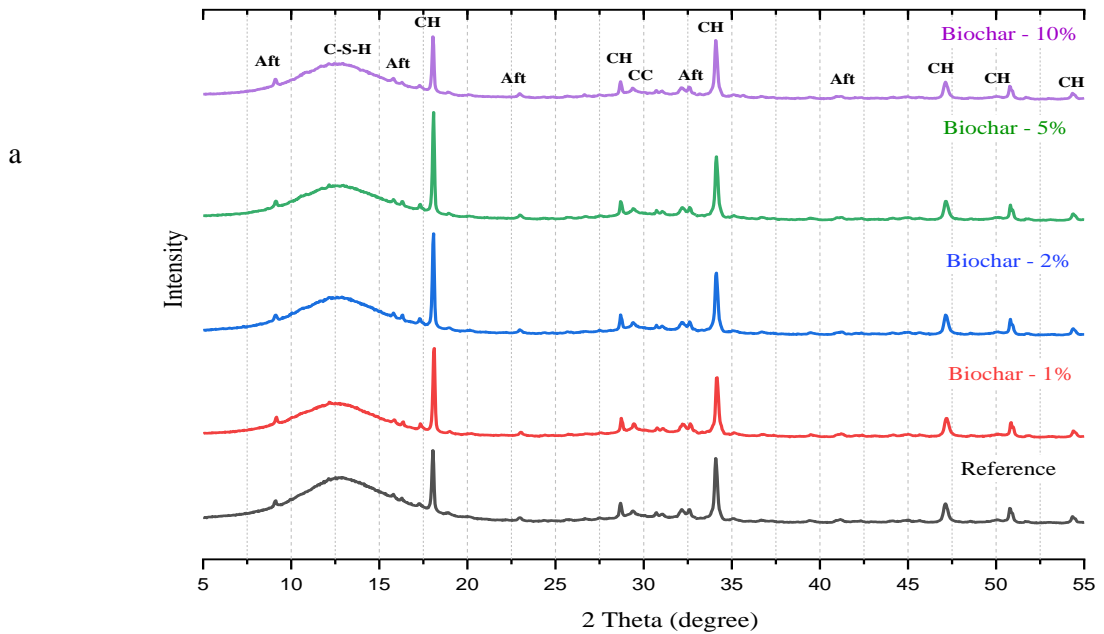
268

269 3.4. Mineralogy of hydration products from sludge biochar composite

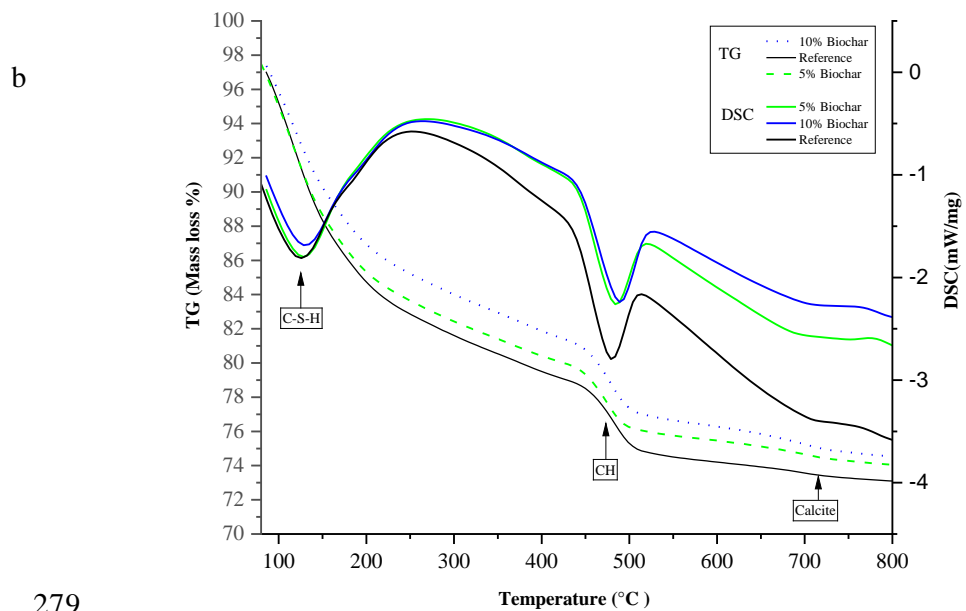
270 The XRD analysis of sludge biochar composite cement paste mixture at 28 days is shown in
 271 **Fig. 4a**. Very similar to mixtures with raw sludge, the incorporation of the sludge biochar did
 272 not create significant new crystalline phases to the composite. All mixtures presented the main
 273 crystalline phases, i.e. calcium silicate hydrate (CSH), ettringite (Aft) and portlandite (CH). A

274 single peak of calcite was detected in all mixtures. It is important to note that there was a slight
 275 decrease in the peak intensity of calcite in mixtures with biochar compared to blends with raw
 276 sludge (Gomes et al., 2020).

277



278



279

280

281 **Figure 4.** (a) XRD of sludge biochar hydrated mixtures. Aft =Etringita, C-S-H =Calcium
 282 silicate hydrate, CH= Portlandite, CC= Calcite. (b) TG-DSC pattern of reference, 5% and
 283 10% of sludge biochar.

284

285 *3.5. Thermogravimetry and differential scanning calorimetry analysis*

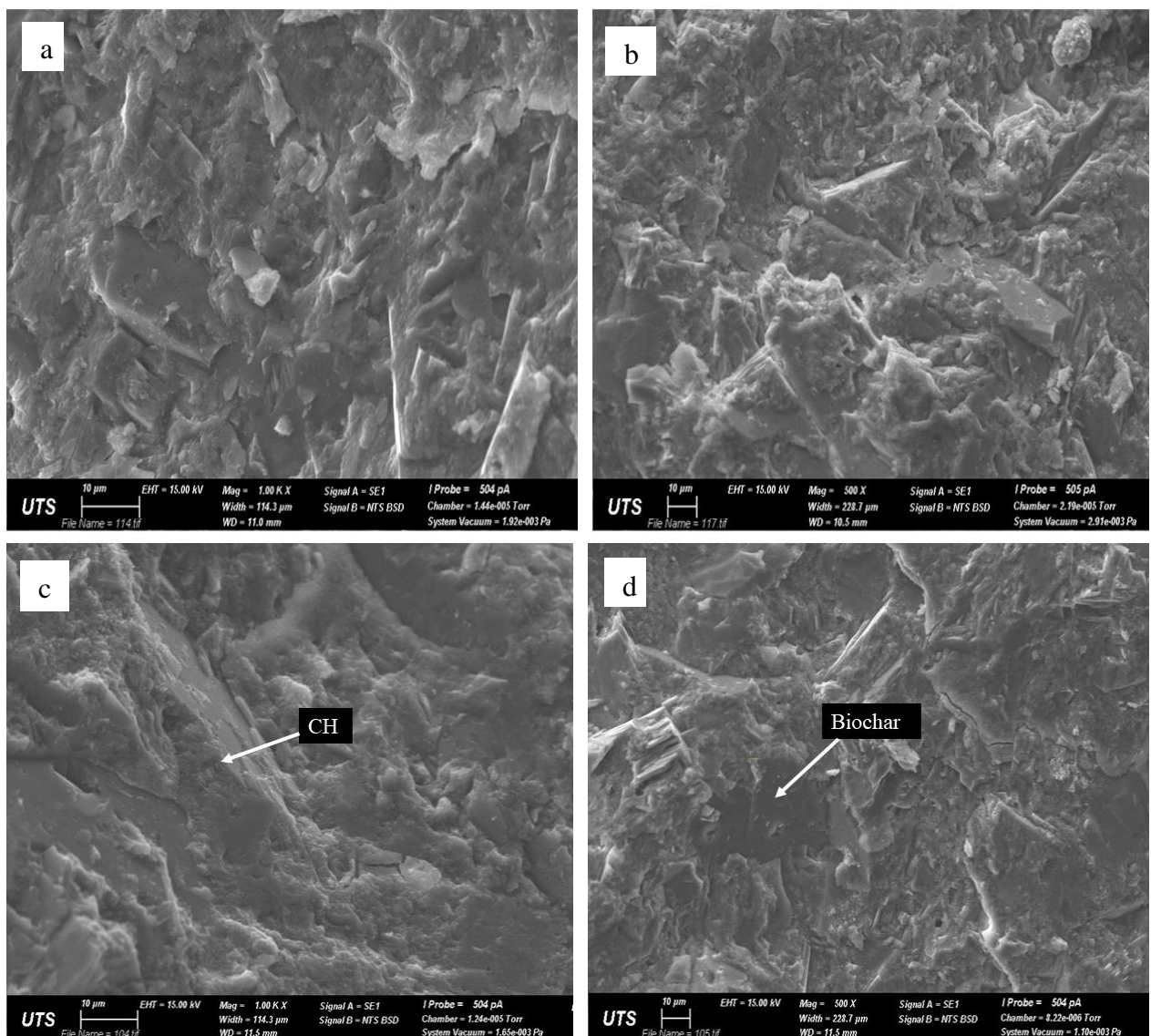
286 To fully understand the effects of sludge biochar on cement paste samples, their chemical
287 composition was examined using TG-DSC. **Figure 4b** shows a comparison of the intensities of
288 portlandite, calcium silicate hydrate (or C-S-H) and calcite between the reference sample, 5%
289 and 10% biochar. Analyzing the first endothermic peak corresponding to C-S-H demonstrated
290 that the cement paste sample with 5% biochar showed similar peak intensity to the reference
291 material, and the sample with 10% biochar had a slightly lower peak intensity compared to the
292 reference sample. The second endothermic peak is related to the calcium hydroxide or
293 portlandite (CH). The results show that all cement paste mixtures, whether with 5% and 10%
294 biochar incorporation, or the reference material, all had a very similar peak intensity. However,
295 when comparing the difference between the intensity of composites with biochar and those with
296 raw sludge, it can be seen that the concentration of C-S-H and portlandite on the biochar
297 composites is very close to the reference material, which does not happen with the samples with
298 raw sludge (Gomes et al., 2020). This is in agreement with the results of mechanical
299 performance, wherein the mixtures with biochar showed compressive strength close to the
300 reference material at 28 days. Unlike the lower intensity of C-S-H and portlandite in the raw
301 sludge composites due to the organic matter, the reason for the lower portlandite peak and
302 compatible compressive strength with biochar is the pozzolanic reaction with the biochar. The
303 consumption of portlandite for the production of extra calcium silicate hydrate (C-S-H) and
304 calcium aluminium silicate hydrate (C-A-S-H) is very common in the presence of pozzolanic
305 materials with a reasonable concentration of metakaolinite (Frias et al., 2013; Mohammed,
306 2017).

307

308 *3.6. Microstructure analysis*

309 The SEM analysis (**Fig. 5**) shows the microstructure of the hydrated composite with additions
310 of 1%, 2%, 5% and 10% biochar. The cement paste mixtures containing 1% and 2% of sludge

311 biochar (**Fig. 5a-b**) showed clearly a well-developed structure with a network of defined
312 hydrated compounds very similar to the reference material. The samples with 5% biochar also
313 presented a clear and dense microstructure very similar to the reference material, with visibly
314 hydrated compounds such as portlandite spread throughout the structure (**Fig. 5c**). For the
315 highest amount of biochar addition (10%), it was possible to observe biochar grains added to
316 the cement paste structure (**Fig. 5d**). In addition, that the structure of the composite with 10%
317 biochar proved to be well developed when compared to the low bond development structure of
318 10% raw sludge (Gomes et al., 2020).



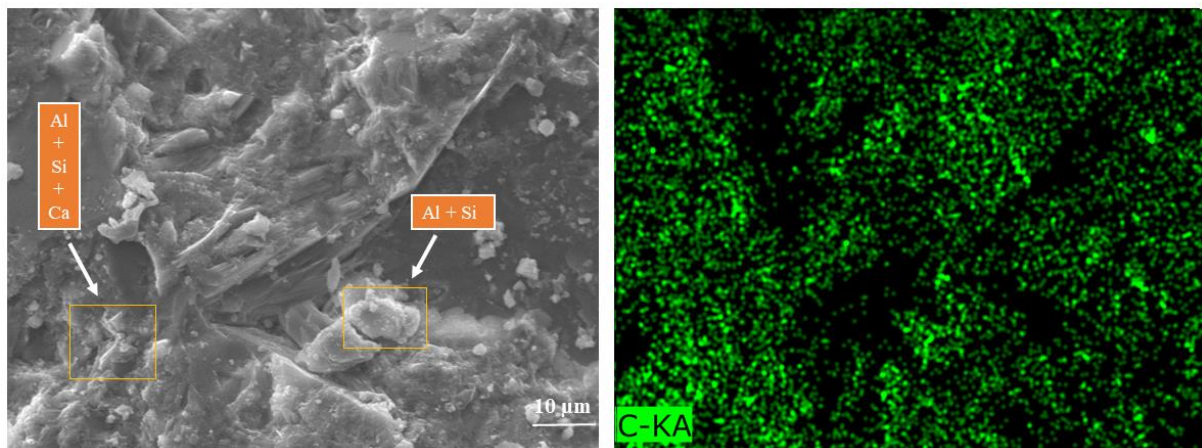
320
321

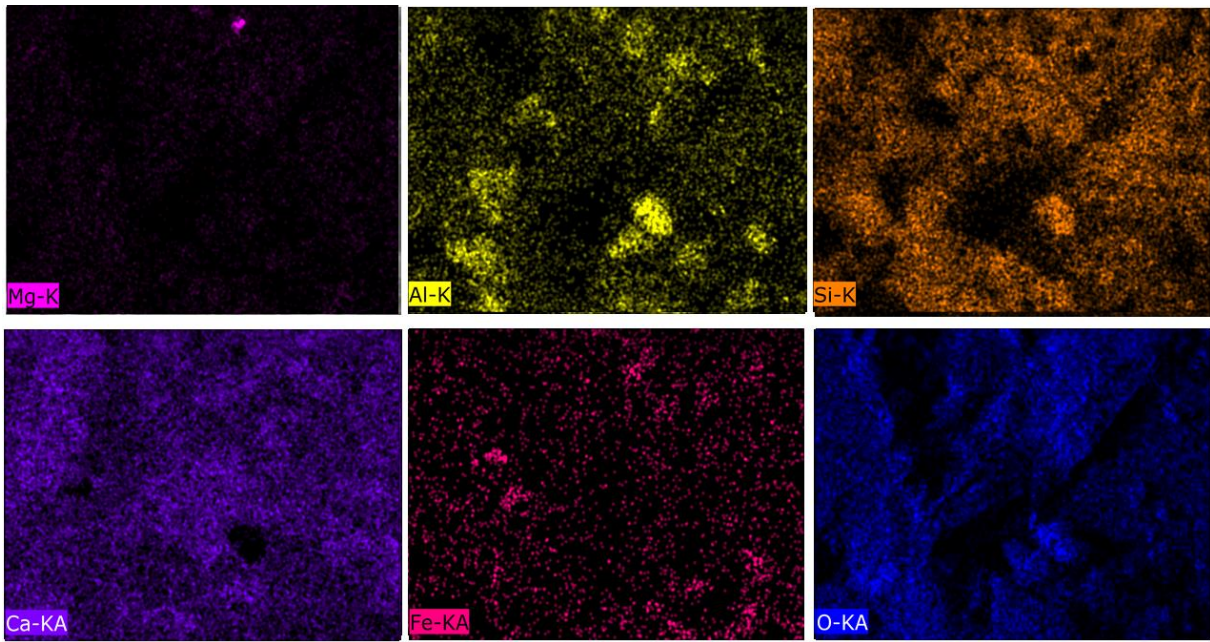
322 **Figure 5.** SEM analysis of hydrated reference cement paste with (a) 1% sludge biochar, (b)
323 2% sludge biochar, (c) 5% sludge biochar, and (d) 10% sludge biochar.

324

325 In order to visualize the element distribution surface of the hardened paste with biochar,
326 elemental mapping using SEM-EDS spectroscopy was carried out. **Figure 6** shows the
327 distribution of the elements for the cement composite samples with 5% biochar at 28 days. The
328 predominant presence of calcium (Ca), oxygen (O) and silica (Si) can be clearly observed,
329 confirming the main cement hydrated compounds of portlandite ($\text{Ca}(\text{OH})_2$) and C-S-H. Another
330 clear observation is the association of aluminium with other elements such as silica, indicating
331 the presence of aluminosilicate particles such as metakaolin. The presence of this pozzolanic
332 material in combination with calcium could lead to the formation of other hydrated products
333 such as C-A-S-H (common in concretes with the addition of metakaolin) visible in the spectrum
334 (Avet et al., 2019)

335





337
338

339 **Figure 6.** SEM-EDS image of the cement paste with 5% of sludge biochar, and its element
340 distribution mapping.

341

342 3.7. Biochar production cost

343 The production of biochar involves several steps such as sample collection (i.e. dewatered
344 sewage sludge), sample preparation (e.g. drying of sewage sludge), pyrolysis, and storage prior
345 to application as a construction material. In addition, transportation is needed to move sludge
346 to the pyrolysis plant, and to move biochar to a construction site. Each of these steps may need
347 capital expenditure (i.e. equipment purchase, depreciation, and insurance), and operating cost
348 such as fuel and labor. The approach by Nematian et al. (2021) was used to estimate itemized
349 cost, on the basis of a mobile pyrolysis unit producing one ton/day of biochar. The calculations
350 are shown in Table 2.

351

352 **Table 2.** Cost of biochar production with one ton/day capacity.

	Unit cost (US\$)	Cost/ton biochar (US\$)
Fixed cost		
Truck	62775	46.84

Trailer and fabrication	30000	25.21
Mobile pyrolysis unit	100000	81.09
Storage shed	20000	13.16
Portable toilet	1270	0.84
Portable septic tank	500	0.33
Fees, permits, and other payments		16.46
<i>Sub total 1</i>		183.93
Variable cost		
Fuel for truck		1.47
Labor		
Pre-processing		42.61
Operations and transportation		127.84
Miscellaneous		
Biochar bags		23.42
Waste disposal		23.42
<i>Sub total 2</i>		195.34
Administrative cost		18.96
<i>Total cost</i>		398.23

353

354 Based on the calculations shown in Table 2, the overall cost of biochar production from
355 sewage sludge will be approximately US\$398.22/ton. The cost is within the range reported for
356 global sales price, from US\$90/ton in the Philippines to US\$8850/ton in the UK, although the
357 average price is US\$2650/ton (Ahmed et al., 2016). Similarly, Nematian et al. (2021) suggested
358 that biochar cost ranged between US\$571 and US\$1455/ton, by converting orchard waste to
359 biochar.

360 Although biochar production from sewage sludge adds some cost, both economic and
361 environmental benefits can be made. If the biochar produced is sold on the market, the cost is
362 likely to be recovered. In addition, biochar production will avoid sending sewage sludge to
363 landfill, which will incur landfill tax (e.g. AU\$147.10/ton in NSW, Australia, £96.70/ton in the

364 UK). The use of sewage sludge-derived biochar as raw materials in construction will
365 undoubtedly bring environmental benefits, and reduce the use of precious natural materials.

366

367 **4. Conclusions**

368 The application of water treatment sludge-derived biochar in cement paste has been tested
369 comprehensively. Water treatment sludge showed a heterogeneous morphology, with various
370 sizes of angular particles and a semi-crystalline/amorphous structure. In comparison, XRD and
371 SEM-EDS analyses of sludge biochar revealed a product with well-defined crystalline phases
372 and pozzolanic material such as methakaline. The thermal process applied to the original sludge
373 has improved hydration heat properties of the cement composites compared to the raw sludge.
374 The composite samples with 2% and 5% of biochar release more heat than the reference
375 samples. After 28 days of curing, the addition of 1-5% biochar in the composite produced a
376 slightly higher compressive strength than the reference material, even 10% biochar addition
377 showed similar compressive strength to the reference material. The results from TG-DSC and
378 SEM-EDS analyses indicate that the reduction of portlandite in the 5% and 10% biochar
379 specimens due to the pozzolanic reaction with biochar. The production of biochar from sewage
380 sludge will be an expenditure, which is reasonable considering the benefits of protecting soil
381 environment and replacing precious natural raw materials in construction industry.

382

383 **Acknowledgements**

384 We acknowledge the financial support from the Endeavour Postgraduate Scholarship,
385 Australia.

386

387 **References**

388 Ahmed, M.B., Johir, M.A.H., Khourshed, C., Zhou, J.L., Ngo, H.H., Nghiem, D.L., Moni, M.,
389 Sun, L., 2018. Sorptive removal of dissolved organic matter in biologically-treated effluent

390 by functionalized biochar and carbon nanotubes: importance of sorbent functionality.
391 Bioresour. Technol. 269, 9-17.

392 Ahmed, M.B., Zhou, J.L., Ngo, H.H., Guo, W., 2016. Insight into biochar properties and its
393 cost analysis. Biomass Bioenerg. 84, 76-86.

394 Akhtar, A., Sarmah, A.K., 2018. Novel biochar-concrete composites: Manufacturing,
395 characterization and evaluation of the mechanical properties. Sci. Total Environ. 616, 408-
396 416.

397 ASTM, 2009. Standard Practice for Measuring Hydration Kinetics of Hydraulic Cementitious
398 Mixtures Using Isothermal Calorimetry. ASTM C1679-09, West Conshohocken, PA, USA.

399 ASTM, 2014. Standard Practice for Mechanical Mixing of Hydraulic Cement Pastes and
400 Mortars of Plastic Consistency. ASTM C305-14, West Conshohocken, PA, USA.

401 ASTM, 2016. Standard Test Method for Compressive Strength of Hydraulic Cement Mortars.
402 ASTM C109-16, West Conshohocken, PA, USA.

403 ASTM, 2020. Standard Test Method for Surface Moisture in Fine Aggregate. Standard C70-20,
404 West Conshohocken, PA, USA.

405 Australian Standard AS 3972, 2010. General Purpose and Blended Cements. Standards
406 Association of Australia, Sydney.

407 Avet, F., Boehm-Courjault, E., Scrivener, K., 2019. Investigation of C-A-S-H composition,
408 morphology and density in limestone calcined clay cement (LC³). Cement Concrete Res.
409 115, 70-9.

410 Beaudoin, J., Odler, I., 2019. Hydration, setting and hardening of Portland cement. In Lea's
411 Chemistry of Cement and Concrete, edited by Hewlett, P.C. and Liska, M., Elsevier, pp.
412 157-250.

413 Beesley, L., Moreno-Jiménez, E., Gomez-Eyles, J.L., 2010. Effects of biochar and greenwaste
414 compost amendments on mobility, bioavailability and toxicity of inorganic and organic
415 contaminants in a multi-element polluted soil. Environ. Pollut. 158(6), 2282-2287.

416 Benlalla, A., Elmoussaouiti, M., Dahhou, M., Assafi, M., 2015. Utilization of water treatment
417 plant sludge in structural ceramics bricks. *Appl. Clay Sci.* 118, 171-177.

418 Cement Australia Pty Limited, 2019. General Purpose Cement - Safety Data Sheet. Australia.

419 Chang, Z., Long, G., Zhou, J.L., Ma, C., 2020. Valorization of sewage sludge in the fabrication
420 of construction and building materials: A review. *Resour. Conserv. Recycl.* 154, 104606.

421 de Godoy, L.G.G., Rohden, A.B., Garcez, M.R., da Costa, E.B., Da Dalt, S., de Oliveira
422 Andrade, J.J., 2019. Valorization of water treatment sludge waste by application as
423 supplementary cementitious material. *Constr. Build. Mater.* 223, 939-950.

424 Di Tommaso, M., Bordonzotti, I., 2016. NO_x adsorption, fire resistance and CO₂ sequestration
425 of high performance, high durability concrete containing activated carbon. In *Book of*
426 *Abstracts volume 192*.

427 Erdogmus, E., Harja, M., Gencel, O., Sutcu, M., Yaras, A., 2021. New construction materials
428 synthesized from water treatment sludge and fired clay brick wastes. *J. Build. Eng.* 42,
429 102471.

430 Frias, M., de la Villa, R.V., García, R., Sánchez de Rojas, M.I., Baloa, T.A., 2013.
431 Mineralogical evolution of kaolin-based drinking water treatment waste for use as
432 pozzolanic material. The effect of activation temperature. *J. Amer. Ceramic Society* 96(10),
433 3188-95.

434 Gomes, S.D.C., Zhou, J.L., Li, W., Long, G., 2019. Progress in manufacture and properties of
435 construction materials incorporating water treatment sludge: A review. *Resour. Conserv.*
436 *Recycl.* 145, 148-159.

437 Gomes, S. D. C., Zhou, J. L., Li, W., Qu, F., 2020. Recycling of raw water treatment sludge in
438 cementitious composites: effects on heat evolution, compressive strength and
439 microstructure. *Resour. Conserv. Recycl.* 161, 104970.2

440 Gupta, S., Kua, H. W., 2017. Factors determining the potential of biochar as a carbon capturing
441 and sequestering construction material: critical review. *J. Mater. Civil Eng.* 29(9),
442 04017086.

443 Gupta, S., Kua, H. W., Koh, H. J., 2018. Application of biochar from food and wood waste as
444 green admixture for cement mortar. *Sci. Total Environ.* 619, 419-435.

445 Hamza, A., John, I.J., Mukhtar, B. 2017. Enhanced photocatalytic activity of calcined natural
446 sphalerite under visible light irradiation, *J. Mater. Res. Technol.* 6(1), 1-6.

447 Huang, X., Wan, Y., Shi, B., Shi, J., 2020. Effects of powdered activated carbon on the
448 coagulation-flocculation process in humic acid and humic acid-kaolin water treatment.
449 *Chemosphere* 238, 124637.

450 Hung, C.-M., Huang, C.-P., Chen, C.-W., Wu, C.-H., Lin, Y.-L., Dong, C.-D., 2020. Activation
451 of percarbonate by water treatment sludge-derived biochar for the remediation of PAH-
452 contaminated sediments. *Environ. Pollut.* 265, 114914.

453 Hussein, A.M., Mahmoud, R.K., Sillanpää, M., Wahed, M.S.A., 2021. Impacts alum DWTPs
454 sludge discharge and changes in flow regime of the Nile River on the quality of surface
455 water and cultivated soils in Fayoum watershed, Egypt. *Sci. Total Environ.* 766, 144333.

456 Kaish, A.B.M.A., Breesem, K.M., Abood, M.M. 2018. Influence of pre-treated alum sludge on
457 properties of high-strength self-compacting concrete. *J. Cleaner Product.* 202, 1085-96.

458 Kakali, G., Perraki, T.H., Tsivilis, S., Badogiannis, E., 2001. Thermal treatment of kaolin: the
459 effect of mineralogy on the pozzolanic activity. *Appl. Clay Sci.* 20(1-2), 73-80.

460 Kizinievič, O., Žurauskienė, R., Kizinievič, V., Žurauskas, R., 2013. Utilisation of sludge waste
461 from water treatment for ceramic products, *Constr. Build. Mater.* 41, 464-73

462 Lee, K.H., Lee, K.G., Lee, Y.S., Wie, Y.M., 2021. Manufacturing and application of artificial
463 lightweight aggregate from water treatment sludge. *J. Clean. Prod.* 307, 127260.

464 Lee, Y.-E., Shin, D.-C., Jeong, Y., Kim, I.T., Yoo, Y.-S., 2020. Pyrolytic valorization of water
465 treatment residuals containing powdered activated carbon as multifunctional adsorbents.
466 *Chemosphere* 252, 126641.

467 Lehmann, J., 2007. A handful of carbon. *Nature* 447 (7141), 143-144.

468 Letshwenyo, M.W., Mokgosi, S., 2021. Investigation of water treatment sludge from drinking
469 water treated with Zetafloc 553I coagulant for phosphorus removal from wastewater. *J.*
470 *Environ. Manage.* 282, 111909.

471 Li, D., Zhuge, Y., Liu, Y., Pham, P.N., Zhang, C., Duan, W., Ma, X., 2021. Reuse of drinking
472 water treatment sludge in mortar as substitutions of both fly ash and sand based on two
473 treatment methods. *Const. Build. Mater.* 277, 122330.

474 Liu, Y., Zhuge, Y., Chow, C.W., Keegan, A., Li, D., Pham, P.N., Huang, J., Siddique, R., 2020.
475 Utilization of drinking water treatment sludge in concrete paving blocks: Microstructural
476 analysis, durability and leaching properties. *J. Environ. Manage.* 262, 110352.

477 Manda, I.K.M., Chidya, R.C.G., Saka, J.D.K., Biswick, T.T., 2016. Comparative assessment of
478 water treatment using polymeric and inorganic coagulants. *Phys. Chem. Earth, Parts A/B/C.*
479 93, 119-29.

480 Mañosa, J., Cerezo-Piñas, M., Maldonado-Alameda, A., Formosa, J., Giro-Paloma, J., Rosell,
481 J.R., Chimenos, J.M., 2021a. Water treatment sludge as precursor in non-dehydroxylated
482 kaolin-based alkali-activated cements. *Appl. Clay Sci.* 204, 106032.

483 Mañosa, J., Formosa, J., Giro-Paloma, J., Maldonado-Alameda, A., Quina, M.J., Chimenos,
484 J.M., 2021b. Valorisation of water treatment sludge for lightweight aggregate production.
485 *Constr. Build. Mater.* 269, 121335.

486 Mohammed, S., 2017. Processing, effect and reactivity assessment of artificial pozzolans
487 obtained from clays and clay wastes: A review. *Constr. Build. Mater.* 140, 10-19.

488 Mulabagal, V., Baah, D.A., Egiebor, N.O., Chen, W.Y., 2017. Biochar from biomass: a strategy
489 for carbon dioxide sequestration, soil amendment, power generation, and CO₂ utilization.
490 Handbook of Climate Change Mitigation and Adaptation, 1937-1974.

491 Nematian, M., Keske, C., Ng'ombe, J.N., 2021. A techno-economic analysis of biochar
492 production and the bioeconomy for orchard biomass. *Waste Manage.* 135, 467-477.

493 Özdemir, Ö., Dunlop, D. J., 2000. Intermediate magnetite formation during dehydration of
494 goethite. *Earth Planet. Sci. Lett.* 177(1-2), 59-67.

495 Rzepa, G., Bajda, T., Gawęł, A., Debiec, K., Drewniak, L., 2016. Mineral transformations and
496 textural evolution during roasting of bog iron ores. *J. Therm. Anal. Calorim.* 123(1), 615-
497 630.

498 San Nicolas, R., Cyr, M., Escadeillas, G., 2013. Characteristics and applications of flash
499 metakaolins. *Appl. Clay Sci.* 83, 253-262.

500 Santos, G.Z., Melo Filho, J.A., Pinheiro, M., Manzato, L., 2019. Synthesis of water treatment
501 sludge ash-based geopolymers in an Amazonian context. *J. Environ. Manage.* 249, 109328.

502 Scrivener, K.L., Juilland, P., Monteiro, P.J., 2015. Advances in understanding hydration of
503 Portland cement. *Cement Concrete Res.* 78,38-56.

504 Shamaki, M., Adu-Amankwah, S., Black, L., 2021. Reuse of UK alum water treatment sludge
505 in cement-based materials. *Constru. Building Mater.* 275, 122047.

506 Steiner, C., Teixeira, W.G., Lehmann, J., Nehls, T. Vasconcelos de Macêdo JL, Blum WEH,
507 Zech W., 2007. Long term effects of manure, charcoal and mineral fertilization on crop
508 production and fertility on a highly weathered Central Amazonian upland soil. *Plant Soil*
509 291:275–290.

510 Taheriyoun, M., Memaripour, A., Nazari-Sharabian, M., 2020. Using recycled chemical sludge
511 as a coagulant aid in chemical wastewater treatment in Mobarakeh Steel Complex. *J. Mater.*
512 *Cycles Waste Manage.* 22, 745-756.

- 513 Tantawy, M.A., 2015. Characterization and pozzolanic properties of calcined alum sludge.
514 Mater. Res. Bullet. 61, 415-421.
- 515 Teixeira, S., Santos, G., Souza, A., Alessio, P., Souza, S., Souza, N., 2011. The effect of
516 incorporation of a Brazilian water treatment plant sludge on the properties of ceramic
517 materials, Appl. Clay Sci. 53(4), 561-5.
- 518 Teodosiu, C., Gilca, A.-F., Barjoveanu, G., Fiore, S., 2018. Emerging pollutants removal
519 through advanced drinking water treatment: A review on processes and environmental
520 performances assessment. J. Cleaner Prod. 197, 1210-21.
- 521 Van Truong, T., Tiwari, D., Mok, Y.S., Kim, D.J., 2021. Recovery of aluminum from water
522 treatment sludge for phosphorus removal by combined calcination and extraction. J. Indust.
523 Eng. Chem. <https://doi.org/10.1016/j.jiec.2021.07.033>
- 524 Yadav, S., Ibrar, I., Altaee, A., Samal, A.K., Ghobadi, R., Zhou, J., 2020. Feasibility of brackish
525 water and landfill leachate treatment by GO/MoS₂-PVA composite membranes. Sci. Total
526 Environ. 745, 141088.